Dyes and Pigments 82 (2009) 147–155

Contents lists available at ScienceDirect

Dyes and Pigments

journal homepage: www.elsevier.com/locate/dyepig

The crystal structures of three azonaphtharylamide pigments

Chia-Hsien Chang [a], Robert M. Christie [b,*], Georgina M. Rosair [c]

[a] National Institute for Materials Science, 1-1 Namiki, Tsukuba City, Ibaraki 305-0047, Japan
[b] School of Textiles and Design, Heriot-Watt University, Scottish Borders Campus, Galashiels TD1 3HF, Scotland, UK
[c] School of Engineering and Physical Sciences, Heriot-Watt University, Edinburgh EH14 4AS, Scotland, UK

ARTICLE INFO

Article history:
Received 28 October 2008
Received in revised form 18 December 2008
Accepted 19 December 2008
Available online 30 December 2008

Keywords:
Azonaphtharylamide
Pigments
X-ray single crystal structure
Polymorphism

ABSTRACT

The single crystal X-ray structures of three structurally related azonaphtharylamide pigments are reported. Two azo pigments derived from 4-amino-3-nitrotoluene as diazo component (**1a** and **b**) crystallize in the centrosymmetric space group $P2_1/c$ while the third (**1c**), an analogue of **1b** but derived from 2,5-dichloroaniline as diazo component, crystallizes in the chiral space group $P2_12_12_1$. The compounds adopt the ketohydrazone tautomeric forms with intramolecular, but no intermolecular, hydrogen bonding. The application performance of the products is discussed in relation to the molecular and crystal structures. X-ray powder diffraction, supported by FTIR spectroscopic and DSC analysis, demonstrate that pigment **1a** shows polymorphism. The application performances of the two polymorphs of this pigment are compared.

1. Introduction

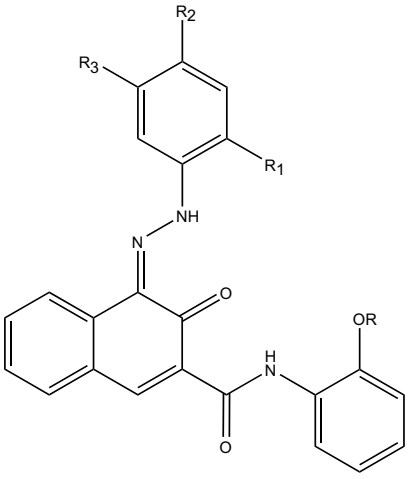

1a (R_1= NO_2, R_2= CH_3, R=OCH_3)

1b (R_1= NO_2, R_2= CH_3, R = OC_2H_5)

1c (R_1= C_l, R_3= Cl, R = OC_2H_5)

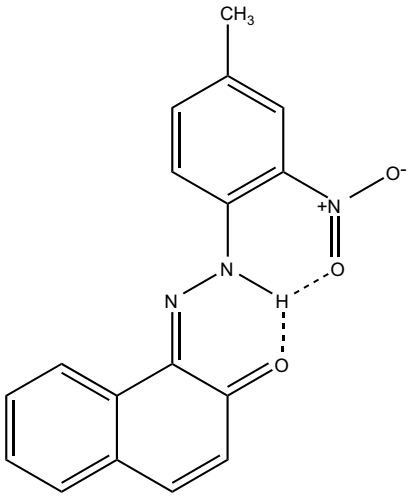

2

The most important red organic pigments are azo pigments obtained from 2-naphthol and its derivatives as coupling components [1–3]. An important subgroup, derived from arylamides of 3-hydroxy-2-naphthoic acid (naphthol AS derivatives)

* Corresponding author.
E-mail address: r.m.christie@hw.ac.uk (R.M. Christie).

0143-7208/$ – see front matter © 2009 Elsevier Ltd. All rights reserved.
doi:10.1016/j.dyepig.2008.12.007

and referred to as azonaphtharylamide oranges and reds, are important industrially for the coloration of paints, printing inks and plastics. Azonaphtharylamide pigments are conveniently classified into two groups. Group 1 products contain a single amide group attached to the naphthol ring. Group 2 pigments are products of superior durability (fastness to light, heat and solvents), achieved by incorporating additional amide or sulphonamide substituents, the technical performance generally improving with the number of such groups present. In a previous paper, we reported the results of a systematic investigation of structure–property relationships in a carefully selected set of Group 1 azonaphtharylamide pigments, derived from either 2,5-dichloroaniline or 4-amino-3-nitrotoluene as the diazo components. This investigation revealed that pigments derived from 2,5-dichloroaniline gave brighter, yellower shades of red and showed superior technical properties, accounting for their greater industrial significance [4]. The enhanced lightfastness, in particular, is at first sight rather surprising on the basis of intramolecular hydrogen bonding arguments as the *o*-chloro group would be expected to show less strong interaction than the *o*-nitro group. The observation contrasts with other series of azo pigments, such as the azonaphthols, of which CI Pigment Red 3 (**2**) is a typical example, which are structurally related but do not contain the arylamide group. It has been clearly demonstrated that pigment **2** shows dramatically improved lightfastness compared with the derivative in which there is no *o*-nitro group [4]. Intramolecular hydrogen bonding involving the *o*-nitro group and the hydrazone N–H is thus proposed as an important feature in enhancing lightfastness properties of the azonaphthols by reducing the electron density at the chromophore and consequently reducing the susceptibility towards photooxidation [1,3]. On the basis of our previous study, an explanation based on molecular structural considerations was proposed to rationalise this observation that in the azonaphtharylamides the ketohydrazone group is provided with a sufficient degree of protection by hydrogen bonding with the amide group. The amide N–H group may in turn become the vulnerable site for photochemical attack. As supporting evidence for this tentative suggestion, electron-releasing groups in the arylide ring, which would be expected to increase the strength of the amide N–H bond, improve lightfastness, while the electron-withdrawing nitro group, which has the opposite effect, decreases lightfastness [4].

Single crystal X-ray crystallographic studies assist understanding of the performance of pigments, which are used in microcrystalline form in their application. The information provided is also fundamentally important to the use of crystal engineering methodology in the design of new products for improved performance. A few single crystal X-ray structures of azonaphtharylamide Group 1 pigments derived from 2,5-dichloroaniline as diazo component have been reported previously [5–7] and the results are discussed in a review article [8]. We have explored the structural features in this series further by determining the X-ray single crystal structures of two azonaphtharylamide pigments **1a** and **b** derived from 4-amino-3-nitrotoluene as diazo component and of pigment **1c**, structurally analogous to **1b** but derived from 2,5-dichloroaniline as diazo component, with a view to understanding whether crystal structural effects contribute towards their application performance. Pigment **1c** indeed shows better colour properties and significantly improved fastness to light, solvents and heat than **1b** [4]. The *o*-methoxy and *o*-ethoxy derivatives were selected as the coupling components because of their presence in two industrially important Group 2 pigments CI Pigments Red 170 and 266, in which there is considerable current interest.

2. Experimental

2.1. Instrumental methods

Infrared spectra of samples were obtained as Nujol mulls (to avoid the potential for polymorphic conversion by grinding with KBr) using a Nicolet Protégé 460 FTIR spectrophotometer. DSC analysis was carried out using a Mettler DSC 30 Differential Scanning Calorimeter connected to a Mettler TC 10 AAT processor with samples of pigment (1.7 mg) heated from 40 °C to 400 °C at a heating rate of 10 min^{-1} under a flowing nitrogen atmosphere. Single crystal X-ray diffraction data were collected on a Bruker AXS P4 four circle diffractometer and X-ray powder diffraction was carried out using a Bruker AXS D-500 diffractometer.

2.2. Synthesis

4-[(2-Nitro-4-methylphenyl)hydrazono]-*N*-(2-methoxyphenyl)-3-oxo-3,4-dihydronaphthalene-2-carboxamide, (**1a**), 4-[(2-nitro-4-methylphenyl)-hydrazono]-*N*-(2-ethoxyphenyl)-3-oxo-3,4-dihydro naphthalene-2-carboxamide, (**1b**) and 4-[(2,5-dichloro)-hydrazono]-*N*-(2-ethoxyphenyl)-3-oxo-3,4-dihydronaphthalene-2-carbo xamide, (**1c**) were synthesized as detailed previously [4]. Samples **1a**′, **b**′ and **c**′ were collected by filtration directly after the coupling reaction at room temperature, followed by freeze-drying. Samples **1a**″, **b**″ and **c**″ were collected by filtration after the aqueous slurries of the pigments were heated at 95–100 °C for 1 h and oven dried at 60 °C. Samples **1a**‴, **b**‴ and **c**‴ were obtained by recrystallisation from toluene. Recrystallisation of pigments to provide samples in sufficient quantity for application testing is impractical. However, the use of organic solvent treatments to effect polymorphic conversion of pigments is common industrial practice [3]. In order to prepare the β-polymorph of **1a** in sufficient quantity and in a form

Table 1
Parameters for the crystal structure determinations for **1a**, **b** and **c**.

Identification code	1a	1b	1c
Empirical formula	$C_{25}H_{20}N_4O_5$	$C_{26}H_{22}N_4O_5$	$C_{25}H_{19}Cl_2N_3O_3$
Formula weight	456.45	470.48	480.33
Crystal system	Monoclinic	Monoclinic	Orthorhombic
Space group	$P2_1/c$	$P2_1/c$	$P2_12_12_1$
Unit cell dimensions	$a = 8.6211(15)$ Å $b = 25.050(5)$ Å $c = 9.692(3)$ Å $\beta = 91.519(14)°$	$a = 8.656(5)$ Å $b = 25.066(5)$ Å $c = 9.966(5)$ Å $\beta = 90.630(5)°$	$a = 3.868(3)$ Å $b = 21.104(4)$ Å $c = 26.023(4)$ Å
Volume	2092.3(8) $Å^3$	2162.2(17) $Å^3$	2124.3(17) $Å^3$
Z	4	4	4
Density (calculated)	1.449 Mg/m^3	1.445 Mg/m^3	1.502 Mg/m^3
Absorption coefficient	0.103 mm^{-1}	0.102 mm^{-1}	0.341 mm^{-1}
Crystal size (mm^3)	$0.72 \times 0.38 \times 0.10$	$0.06 \times 0.56 \times 0.38$	$0.82 \times 0.12 \times 0.04$
Theta range for data collection	2.25–25.00°	2.20–25.00°	1.84–25.01°
Index ranges	$-1 \le h \le 10$ $-29 \le k \le 1$ $-11 \le l \le 11$	$-10 \le h \le 1$ $-1 \le k \le 29$ $-11 \le l \le 11$	$-1 \le h \le 4$ $-1 \le k \le 25$ $-1 \le l \le 30$
Reflections collected	4655	4772	3136
Independent reflections, R(int)	3667, 0.0525	3769, 0.0718	2250, 0.1089
Completeness to theta = 25.00°	99.3%	98.8%	99.1%
Absorption correction	Psi-scans	None	None
Max. and min. transmission	0.8436, 0.7566	0.955,0.994	0.952,0.986
Data/restraints/parameters	3667/0/317	3769/0/324	2250/2/305
Goodness-of-fit on F^2	1.028	1.055	1.063
Final R indices [$I > 2\sigma(I)$] $R1$, $wR2$	0.0514, 0.1236	0.0679, 0.1730	0.0778, 0.2067
R indices (all data) $R1$, $wR2$	0.0774, 0.1384	0.1312, 0.2129	0.1355, 0.2926
Largest diff. peak and hole e $Å^{-3}$	0.226 and −0.337	0.364 and −0.476	0.815 and −0.970

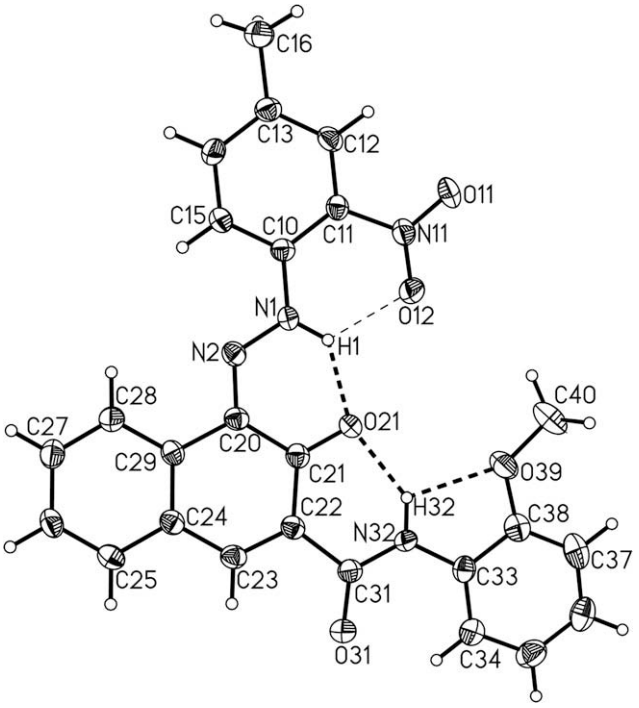

Fig. 1. Molecular structure of **1a** with 50% probability displacement ellipsoids (intramolecular hydrogen bonds indicated).

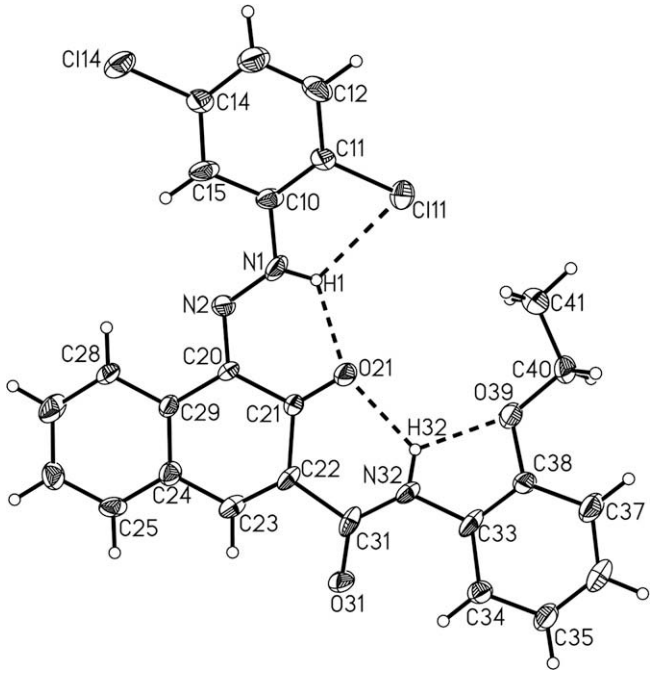

Fig. 3. Molecular structure of **1c**, with 50% probability displacement ellipsoids (intramolecular hydrogen bonds indicated).

suitable for testing in paint application, a sample of **1a** (10 g) was heated at reflux with stirring in toluene (100 cm^3) for 1 h, filtered and oven dried at 60 °C. This sample was demonstrated by powder X-ray diffraction and FTIR spectrum to be in the β-form.

Incorporation of the pigments into printing ink and industrial paint systems and assessment of technical properties were carried out as previously described [4].

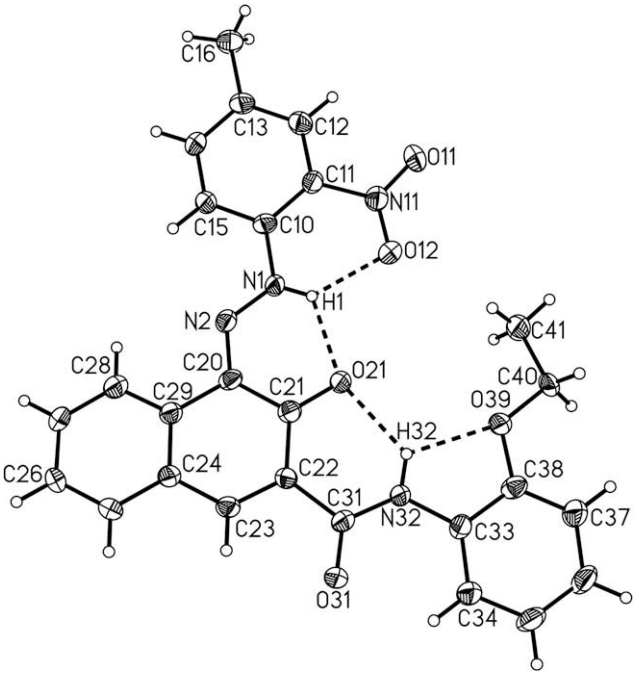

Fig. 2. Molecular structure of **1b**, with 50% probability displacement ellipsoids (intramolecular hydrogen bonds indicated).

2.3. Crystal data

Crystals suitable for X-ray analysis were obtained by slow cooling of a solution of the pigments in toluene, contained in a tube sealed under vacuum from a starting temperature of 100 °C. The single crystals were covered in Nujol and mounted with vacuum grease on a glass fibre on a Bruker AXS P4 diffractometer [9]. Data were collected with MoK_α radiation (0.7107 Å) at 160 K cooled by an Oxford Cryosystems Cryostream. No significant crystal decay was found. Data were corrected for adsorption by psi scans (**1a**). Absorption correction was attempted on **1c** but it did not improve the model. The structures were solved by direct and difference Fourier methods and refined by full-matrix least-square on F^2. All non-hydrogen atoms were refined with anisotropic displacement parameters. Crystallographic computing was performed with SHELXTL [10] and PLATON [11] programs. H atoms bound to N or O atoms were located in the difference Fourier map, their coordinates freely refined and their displacement parameters treated as riding on the bound atom. Further details are given in Table 1.

Table 2
Selected geometric parameters for compounds **1a**, **b** and **c** (Å, °).

	1a	1b	1c
N(1)–N(2)	1.319(3)	1.311(4)	1.322(13)
N(1)–C(10)	1.397(3)	1.417(5)	1.411(13)
N(2)–C(20)	1.323(3)	1.320(5)	1.337(12)
C(21)–O(21)	1.253(3)	1.260(5)	1.227(12)
C(31)–O(31)	1.236(3)	1.233(4)	1.237(13)
C(31)–N(32)	1.347(3)	1.353(5)	1.324(14)
N(32)–C(33)	1.410(3)	1.421(5)	1.430(12)
C(38)–O(39)	1.371(3)	1.373(4)	1.387(12)
O(39)–C(40)	1.425(3)	1.426(4)	1.441(14)
O(39)–C(40)–C(41)		107.2(3)	107.3(9)
N(1)–N(2)–C(20)–C(21)	0.4(3)	−0.4(6)	−1(2)
N(2)–C(20)–C(21)–O(21)	−3.9(3)	−2.2(6)	1.1(19)
O(21)–C(21)–C(22)–C(31)	−1.7(3)	−6.7(6)	−4.2(19)
C(21)–C(22)–C(31)–N(32)	−5.6(3)	−5.2(6)	3.6(16)
N(32)–C(33)–C(38)–O(39)	−1.3(3)	−1.5(5)	−5.2(19)
C(38)–O(39)–C(40)–C(41)		161.2(4)	175.0(12)

Table 3
Hydrogen bonds for compounds **1a**, **b** and **c** (Å, °).

D–H…A	**1a**	**1b**	**1c**	**1a**	**1b**	**1c**	**1a**	**1b**	**1c**	**1a**	**1b**	**1c**
	d (D–H)			*d* (H…A)			*d* (D…A)			<(DHA)		
N(1)–H(1)…O(21)	0.93(3)	0.85(4)	0.91(2)	1.84(3)	2.02(4)	2.03(11)	2.568(2)	2.609(4)	2.575(10)	134(2)	126(4)	117(10)
N(1)–H(1)…O(12)	0.93(3)	0.85(4)		2.04(3)	2.01(4)		2.646(2)	2.637(4)		122(2)	129(4)	
N(1)–H(1)…Cl(11)			0.92(9)			2.50(12)			2.947(11)			110(9)
N(32)–H(32)…O(21)	0.90(3)	0.88(4)	0.90(2)	1.94(3)	2.11(4)	2.12(10)	2.684(3)	2.741(4)	2.723(10)	140(2)	128(4)	0123(9)
N(32)–H(32)…O(39)	0.90(3)	0.88(4)	0.92(10)	2.13(3)	2.09(4)	2.08(10)	2.579(3)	2.609(4)	2.617(12)	110(2)	117(3)	116(8)

3. Results and discussion

Figs. 1–3 show the molecular structures with numbering systems of compounds **1a**, **b** and **c**, respectively.

There are distinct similarities in the crystal structures of **1a** and **b**, not unexpectedly in view of the strong similarities between the molecular structures. Both pigments crystallize in the common centrosymmetric space group $P2_1/c$ and have very similar unit cell dimensions. Pigment **1c** crystallizes differently in $P2_12_12_1$. In common with all crystal structures of commercial azo pigments that have been reported previously [2,12], all three compounds exist in the ketohydrazone tautomeric form. The N(1)–N(2), N(2)–C(20) and C(21)–O(21) bond lengths, similar in magnitude to the corresponding bond lengths in previously determined structures of Group 1 azonaphtharylamide pigments, can be used to confirm this arrangement in **1a**, **b** and **c** (Table 2)[8].

Pigment **1c** shows improved fastness to light compared with **1b** in spite of the fact that an *o*-chloro group might be expected to provide weaker intramolecular hydrogen bonding than the *o*-nitro group. This is a consistent trend which we have previously confirmed in the azonaphtharylamide pigments series [4]. Based on molecular structural considerations, we previously proposed the explanation that, in the azonaphtharylamides, the ketohydrazone group is provided with sufficient protection by intramolecular hydrogen bonding with the amide C═O and that the amide N–H group may become the vulnerable site for photochemical attack. As supporting evidence for this suggestion, electron-releasing groups in the arylide ring, which would be expected to increase the strength of the amide N–H bond, improve lightfastness while electron-withdrawing groups decreases lightfastness [4]. From the X-ray crystal structure data of pigments **1a**, **b** and **c**, intramolecular hydrogen bonds are observed which are bifurcated at the acceptor end. Interatomic distances indicate strong hydrogen bonding between hydrazone atom H(1) and keto atom O(21), and between atom O(21) and secondary amide atom H(32) (Table 3). As a result, the strong hydrogen bonds involving atom O(21) probably contribute to the lengthening of the C═O bond. There is also a weaker interaction between atom H(32) and atom O(39) (methoxy in **1a** and ethoxy in **1b** and **c**). In **1a** and **b**, the nitro group engages in hydrogen bonding with just one of the O atoms, O(12) with the hydrazone H(1). However, the difference in N–O bond lengths between the two O atoms is barely significant, in fact insignificant for **1b** [1.228(4) cf. 1.230(4) Å]. There is also little difference in the phenyl C–C distances which suggests that the 'resonance assisted hydrogen bonding' involving nitro groups noted elsewhere [13] is not significant in the case of pigments **1a** and **b**. This provides support for the proposition that intramolecular hydrogen bonding involving the nitro group does not play a major role in determining lightfastness in the azonaphtharylamide pigments. This contrast with the azonaphthol pigments, such as CI Pigment Red 3 (**2**), in which the presence of the *o*-nitro group provides a significant improvement in lightfastness. In the crystal structure of **2**, the N–O bond which is hydrogen-bonded to the hydrazone H is lengthened, 1.230(5) Å [cf 1.215(6) Å] for the non-hydrogen bonded N–O), and there are greater differences in the phenyl ring C–C bond lengths and, although these differences are small, they are indicative of some resonance-assisted hydrogen bonding [14].

In contrast to the crystal structures of Group 2 azonaphtharylamide pigments, there is no intermolecular hydrogen bonding observed in **1a**, **b** and **c**. The X-ray crystal structures of CI Pigment Red 208, [15] which contains a benzimidazolone group, and CI Pigments Red 266 [16] and 170 [17], both of which contain a primary amide group, have demonstrated that they form layers of molecules with a two-dimensional network of intermolecular hydrogen bonds. This feature is principally responsible for the superior durability of these pigments.

In the solid state, **1a**, **b** and **c** all deviate slightly from planarity, with the phenylhydrazone and anilide rings both twisted slightly with respect to the naphthol plane. The rms deviation of the

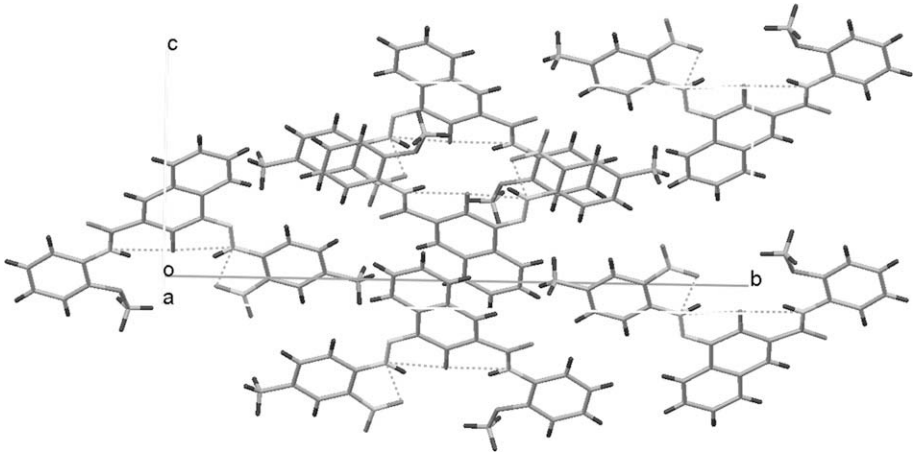

Fig. 4. Molecular packing of **1a** viewed down the *a*-axis.

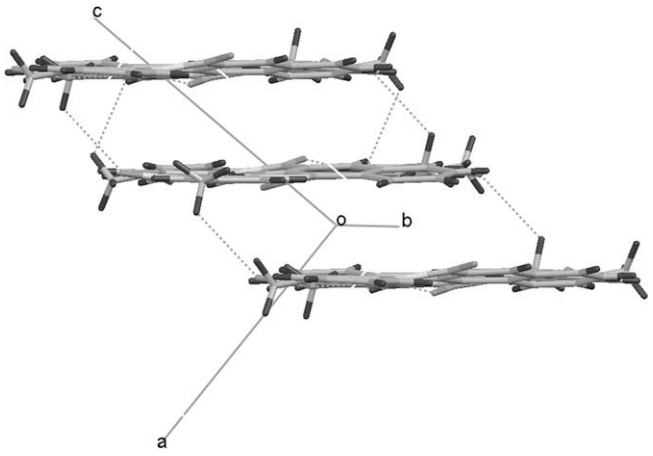

Fig. 5. Molecular packing of **1a** viewed down the *b*-axis.

molecular plane defined by all the non-H atoms are 0.176(4), 0.119(2) and 0.148(11) Å in the case of **1a**, **b** and **c** respectively. The amide O, O31, deviates the most [0.444(3) Å **1a**, 0.346(2) Å, **1b**] from this plane for both molecular species and it is also the only electronegative atom not to be involved in short hydrogen bonds (Table 3). In **1c** (discounting the ethyl group) Cl(14) deviates the most [0.238(4) Å] from the molecular plane.

Compounds **1a** and **b** adopt similar packing patterns (Figs. 4–9). **1a** forms layers which lie parallel to the *b*-axis but inclined at between 40 and 50° to both the *a* and *c* axes. O(31) makes a C–H…O hydrogen bond with H(14) (2.29 Å) within the layers as the shortest intermolecular interaction whilst in **1b** it is a C–H…H–C distance which is the shortest (2.25 Å) for C(41)–H(41B)…H(25)–C(25). This interaction involves the ethyl group (cf., methyl in **1a**) and suggests that increasing the size of this alkyl substituent further might radically change the packing arrangement, considering that an H…H distance is the closest and usually repulsive, compared to C–H…O contacts which are largely attractive. There are few if any H…H distances below 2.2 Å [16]. In **1b** O(31) is 2.41 Å to H(14) within layers whilst between the layers H(40C) is 2.69 Å from O(12) in **1a** and in **1b** O(31)…N(11) is 2.974(5) Å. Similarly between the layers there is a C–H π-interaction (2.64 Å, **1a** and 2.63 Å in **1b**) with the ring C(24)–C(29) and a methoxy H on C(40). The molecules do not stack directly on top of each other and there are no centroid – centroid distances less than 3.731(2) Å (**1a**), 3.769(3) Å (**1b**). Viewing down the *a*-axis (Fig. 4, **1a**; Fig. 7, **1b**) shows that the molecules form layers and these layers are orientated anti-parallel with respect to each other, as seen in the *b*-axis projection (Fig. 5, **1a**; Fig. 8, **1b**).

In **1c**, the molecules pack as columns composed of two stacks in a herringbone arrangement. This is very different to **1a** and **b**. The two stacks which form the herringbone column meet where O(31) is 2.41 Å from H(12) in the neighbouring stack (Fig. 10). The view directly down these stacks (down the *a*-axis) is shown in Fig. 11.

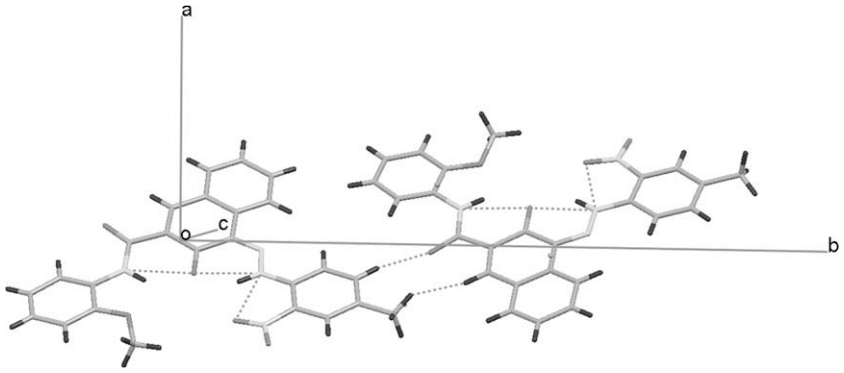

Fig. 6. Molecular packing of **1a** viewed down the *c*-axis.

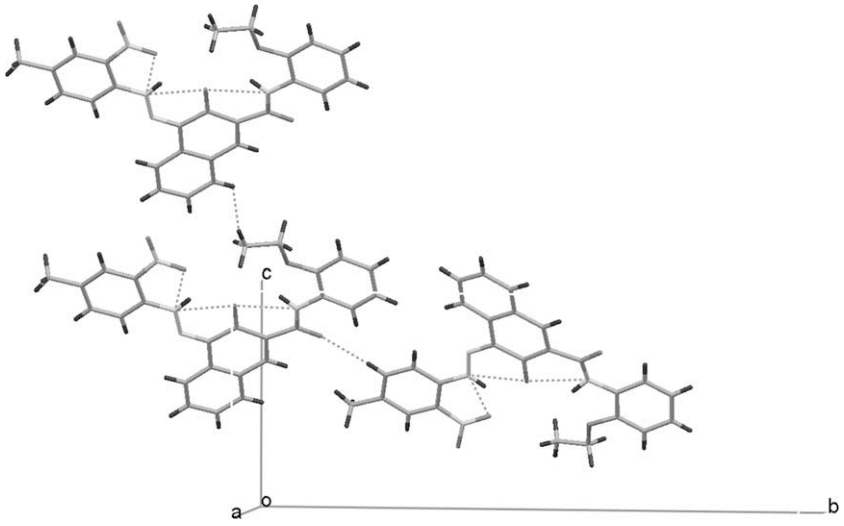

Fig. 7. Molecular packing of **1b** viewed down the *a*-axis.

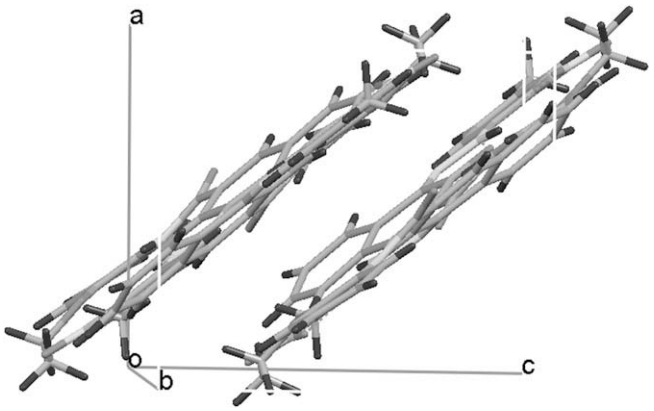

Fig. 8. Molecular packing of **1b** viewed down the *b*-axis.

Within the stacks the shortest C–X…π-interaction of 3.503(11) Å is between C(21)–O(21) and the ring C(20)…C(29) centroid at $x+1$, y, z. The molecules overlap a little more closely than **1a** and **b** with the closest centroid to centroid distance 3.649(7) Å between rings C(20)–C(29) and C(24)–C(29) at $x+1$, y, z. Between neighbouring columns, on the opposite side of the molecule to O(31) there is a CH…Cl contact of 2.86 Å [C(28)–H(28)…Cl(14)]. This intermolecular interaction and the stronger π-stacking arrangement may provide an explanation for the enhanced solvent resistance of **1c** compared with **1b**, possibly also contributing towards its enhanced lightfastness [4].

X-ray powder diffraction (Fig. 12) and FTIR spectra demonstrate that pigment **1a** exhibits polymorphism. Azo pigments are prepared by an azo coupling reaction carried out in water, generally at ambient temperature, subsequently heated to boiling to induce crystallization, which generally provides enhanced colouristic and technical performance [4]. Pigment **1a** precipitated directly from the coupling reaction without heat treatment (sample **1a**′) is

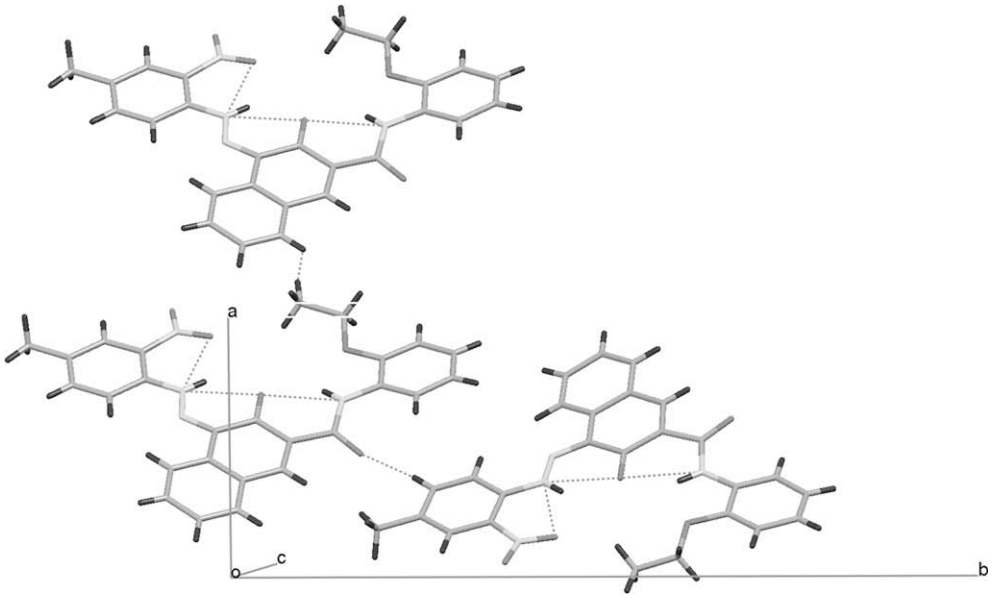

Fig. 9. Molecular packing of **1b** viewed down the *c*-axis.

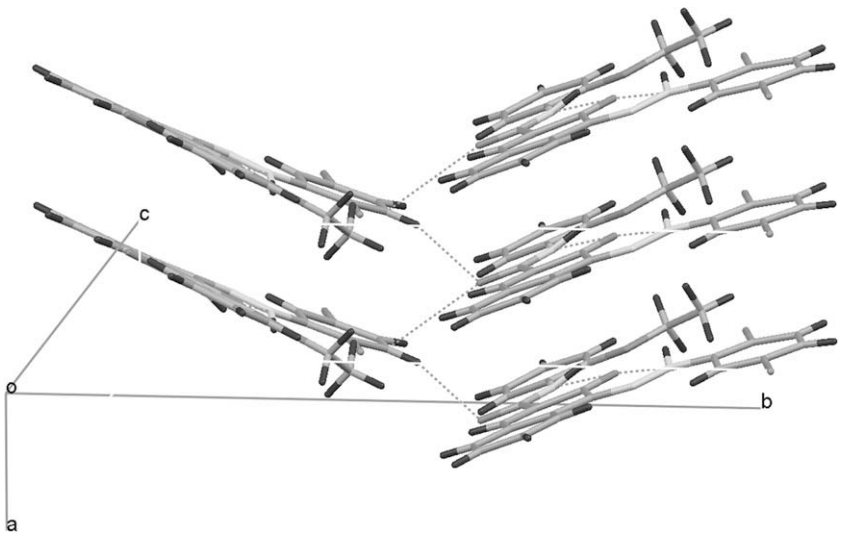

Fig. 10. Herringbone arrangement in **1c**.

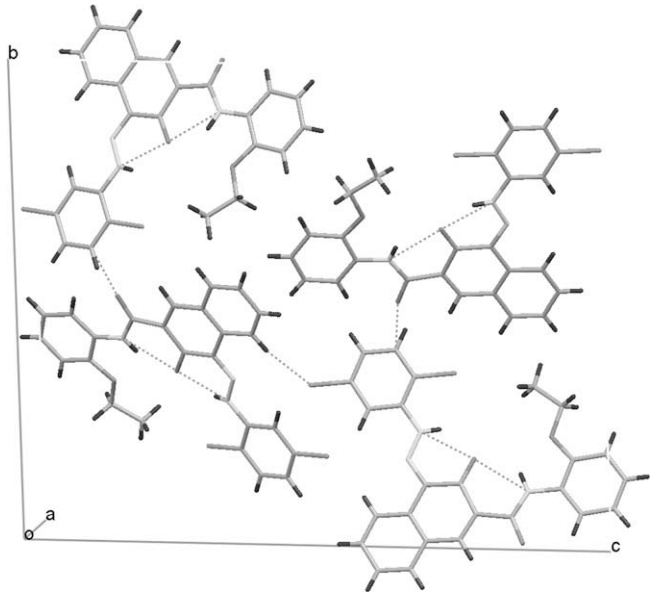

Fig. 11. Molecular packing of **1c** viewed down the *a*-axis.

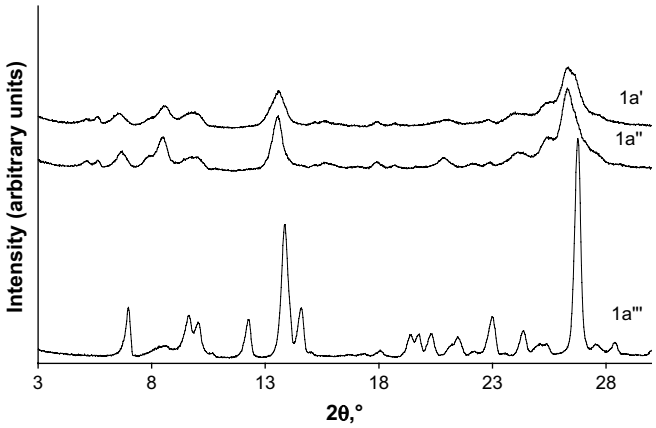

Fig. 12. X-ray powder diffraction traces for samples of pigment **1a**.

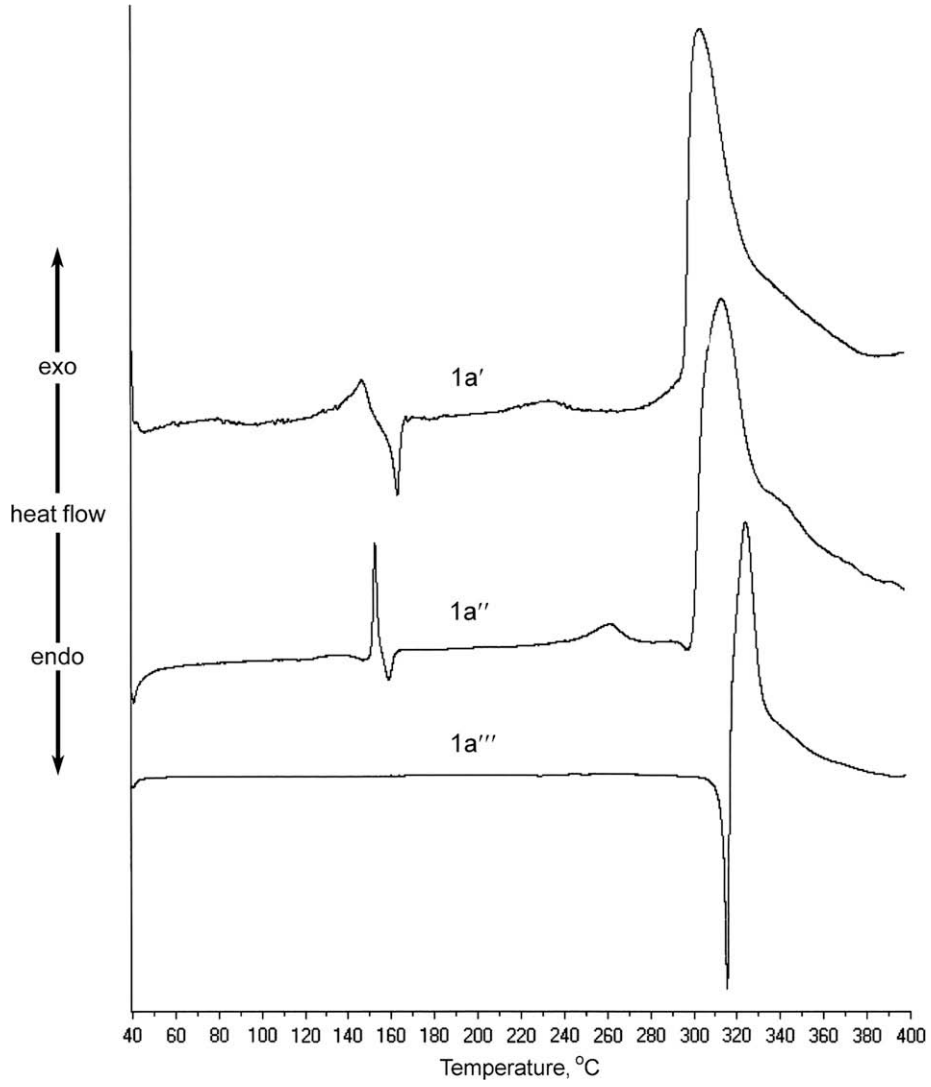

Fig. 13. DSC thermograms of samples of pigment **1a**.

weakly crystalline in a form denoted as the α-form (Fig. 12). The XRD trace for aqueous heat-treated sample **1a**″ shows peaks in the same positions but with improved definition, indicating that it exists in the α-form with crystallinity enhanced by the heat treatment process. A sample recrystallised from toluene (**1a**‴) is highly crystalline and the significantly different powder XRD pattern confirms the formation of a different polymorphic form, denoted as the β-form. The crystal structure of **1a** reported in this paper, obtained from a sample recrystallised from toluene is of the β-form. This was confirmed by synthesis of the powder pattern [18] from the single crystal diffraction data for **1a**, which most closely matches the powder pattern of the β-form, in particular the intense peak at 27.2° in 2θ. The FTIR spectra provide conformation of the polymorphism. The spectra of **1a**′ and **1a**″ are essentially identical, while there are differences throughout the spectrum of **1a**‴. As an example, the secondary amide carbonyl stretching vibration is shifted to lower frequency (1667 cm^{-1}) in the β-form compared with the α-form (1671 cm^{-1}).

DSC was used to provide evidence for the polymorphic transformations in samples of pigment **1a** (Fig. 13). Samples **1a**′ and **1a**″ show initial exotherms between 146 and 152 °C probably due to recrystallisation of the α-form to higher crystallinity. In both cases this is followed by an endotherm (159–163 °C). This is attributed to an α → β solid state transition. FTIR spectra of α-form samples **1a**′ and **1a**″ heated at 165 °C for 20 min conclusively demonstrated conversion to the β-form. Exotherms at 232 °C and 262 °C respectively are probably due to recrystallisation of the β-form to higher crystallinity. The irreversibility of each of these solid state transitions was confirmed by heating/cooling cycle DSC experiments. These involved consecutive sequences of heating the samples to a temperature at which the particular transition was complete, cooling back to room temperature and then reheating to the next transition. In each case, there was no DSC peak in the opposite sense on cooling and the exotherm or endotherm due to the particular transition was not present on reheating. Neither of these two samples showed clear melting behaviour, but there is a large high temperature decomposition exotherm. Visual observation of the samples examined by hot-stage microscopy over the same temperature range was consistent with these conclusions. The highly crystalline sample **1a**‴ shows no solid state transitions. It provides an endothermic melting peak with an extrapolated onset temperature of 307 °C, followed immediately by exothermic decomposition. These results suggest that the β-form is the thermodynamically more stable form, while the α-form is metastable. Pigment **1b** shows more complex polymorphic behaviour. XRD traces and FTIR spectra are sufficiently different to demonstrate that samples **1b**′, **b**″ and **b**‴ exist in three different forms, denoted as α-, β- and γ-forms respectively. The DSC behaviour of the samples of **1b** is very complex and has not been investigated in detail. There is no clear evidence for polymorphism in the case of **1c**.

It was found that treatment of **1a** as a concentrated slurry in toluene at reflux for 1 h effected the polymorphic conversion enabling preparation of a pigmentary sample of the β-form. The results of a colouristic assessment in a lithographic printing ink and a technical assessment of the two polymorphic forms of the pigment in industrial paints are given in Tables 4 and 5 respectively. The β-form, obtained by solvent treatment, is colouristically more interesting, having higher lightness (L) and chroma (C^*) values, and is yellower (higher b^* value). The α-form gives a rather dull bluish-red. Solvent resistance is assessed by controlled overspraying of a dried full-strength paint with a white paint and is quantified as the colour difference (ΔE) between this film and the white film. Both polymorphs show considerable colour bleed in this application, at an identical level, consistent with the absence of significant intermolecular interactions in the crystal structure. The lightfastness (350 h Xenotest exposure) of the β-form is marginally better than the α-form both in a full strength and white reduced paints which may be related to a change in crystal arrangement, or alternatively to crystal growth and improved definition as a result of the solvent treatment process. The most significant difference in properties is the enhanced thermal stability of the β-form at 160 °C. The α-form shows good heat stability to 140 °C but very significant colour change at 160 °C, probably due to polymorphic conversion in application at this temperature.

Table 4
Colouristic values for the α- and β-forms of **1a** in lithographic printing inks [4].

Pigment	L	a^*	b^*	C^*
1a (α-form)	59.6	23.2	−4.7	23.6
1a (β-form)	69.6	26.1	2.7	26.2

Table 5
Technical performance of α- and β-forms of **1a** incorporated into industrial paints, expressed as colour difference (ΔE) before and after the test [4].

Pigment	Overspray fastness[a]	Heat stability[b] 120, 140, 160 °C	Light fastness[b] (full strength)	Light fastness[b] (white reduction)
1a (α-form)	6.4	0.8, 0.8, 18.2	3.8	3.4
1a (β-form)	6.4	1.5, 1.5, 1.6	3.5	2.8

[a] Thermosetting acrylic.
[b] Air-drying alkyd paint.

4. Conclusion

The crystallographic arrangements of three structurally related Group 1 azonaphtharylamide pigments have been determined by single crystal X-ray crystallography. The application performance of the pigments, including lightfastness and solvent resistance, has been correlated with features of the molecular structure and the crystal packing arrangement. The crystal structures of **1a** and **b** indicate the absence of significant resonance-assisted intramolecular hydrogen bonding involving the *o*-nitro groups, consistent with observation that this group apparently does not enhance lightfastness in application. Enhanced intermolecular interactions and more pronounced π–π stacking may explain the improved technical performance of pigment **1c**. Pigment **1a** undergoes a polymorphic transformation when treated with toluene. The new β-polymorph has significantly improved colouristic properties compared with the α-form, and marginally better technical performance.

Acknowledgement

The authors thank Dominion Colour Corporation, Toronto, Canada, for financial support and for carrying out application testing. Thanks are due in particular to Dr Mark Vincent for helpful discussion.

References

[1] Christie RM. Colour chemistry. Cambridge: Royal Society of Chemistry; 2001 [Chapter 9].
[2] Christie RM. The organic and inorganic chemistry of pigments. London: Oil and Colour Chemists' Association; 2002.
[3] Herbst W, Hunger K. Industrial organic pigments. Firstst edition. Weinheim/Cambridge: VCH; 1993;
Herbst W, Hunger K. Industrial organic pigments. Second edition. Weinheim/Cambridge: VCH; 1997;
Herbst W, Hunger K. Industrial organic pigments. Third edition. Weinheim/Cambridge: VCH; 2004.

[4] Christie RM, Chang CH, Huang HY, Vincent M. Colour & constitution relationships in organic pigments: Part 6. Azonaphtharylamide pigments. Surf Coat Int Part B: Coat Transact 2006;89:77–85.
[5] Kobelt D, Paulus EF, Kunstmann W. Röntgeneinkristallstrukturanalyse von 1-(2,5-Dichlorphenylazo)-2-hydroxy-3-naphthoesäure-(4-chlor-2,5-dimethox yanilid) (Chlorderivat von Permanentbraun FG). Acta Crystallogr 1972;B28:1319–24.
[6] Kobelt D, Paulus EF, Kunstmann W. Röntgeneinkrystallstrukturanalyse eines Chlorderivates von Permanentrot FRLL. Vergleich mit dem entsprechenden derivat von Permanentbraun FG. Z Kristallogr 1974;139:15–32.
[7] Whitaker A. The crystal structure of CI Pigment Red 2, 1′-(2,5-dichlorophenyl)azo-2′-hydroxy-3′-phenylamidonaphthalene. Z Kristallogr 1977;146:173–84.
[8] Whitaker A. Crystal structure analysis of azo pigments involving β-naphthol: a review. J Soc Dyers Color 1978;69:431–5.
[9] Siemens. XSCANS. Version 2.2. Madison, Wisconsin, USA: Siemens Analytical X-ray Instruments Inc.; 1996.
[10] Bruker. SHELXTL. Version 5.1. Madison, Wisconsin, >USA: Bruker AXS Inc.; 1999.
[11] Spek AL. PLATON. J Appl Crystallogr 2003;36:7–13.
[12] Hunger K. The effect of crystal structure on colour application properties of organic pigments. Rev Prog Color 1999;29:71–84.
[13] Szczesna B, Urbanczyk-Lipkowska Z. Cooperative effect of multiple hydrogen bonding involving the nitro group: solid state dimeric self-assembly of *o*-, *m*- and *p*-hydroxyphenyl-2,4-dinitrophenylhydrazones. New J Chem 2002;26:243–9.
[14] Whitaker A. The crystal structure of CI Pigment Red 3, 4-methyl-2-nitrophenylazo-2-naphthol. Z Kristallogr 1978;147:99–112.
[15] Paulus EF, Hunger K. Über die Molekül- und Kristallstruktur eines roten Mono-''azo''-pigmentes. Farbe Lack 1980;86:116–20.
[16] Chang CH, Christie RM, Rosair Gm. CI Pigment Red 266. Acta Crystallogr 2003;C59:556–8.
[17] Schmidt MU, Hofmann DWM, Buchsbaum C, Metz HJ. Crystal structures of Pigment Red 170 and derivatives, determined by X-ray powder diffraction. Angew Chem Int Ed 2006;45:1313–7.
[18] Yvon K, Jeitschko W, Parthe E. Lazy Pulverix, a computer program, for calculating X-ray and neutron diffraction powder patterns. J Appl Crystallogr 1977;10:73–4.